

Semileptonic Decays: an Update Down Under*

James N. Simone

Theory Group, Fermilab, P.O. Box 500, Batavia, IL, 60510, USA

Heavy-meson semileptonic decays calculations on the lattice are reviewed. The focus is upon obtaining reliable matrix elements. Errors that depend upon the lattice spacing, a , are an important source of systematic error. Full $O(a)$ improvement of matrix elements for arbitrary-mass four-component quarks is discussed. With improvement, bottom-quark matrix elements can be calculated directly using current lattices. Momentum dependent errors for $O(a)$ -improved quarks and statistical noise limit momenta to around 1 GeV/c with current lattices. Hence, maximum recoil momenta can be reached for D decays while only a fraction of the maximum recoil momentum can be reliably studied for the light-meson decay modes of the B . Differential decay rates and partial widths are phenomenologically important quantities in B decays that can be reliably determined with present lattices.

1. INTRODUCTION

Semileptonic decays provide much needed information about CKM matrix elements involving heavy quarks. Precise CKM values are important for finding the origin of CP violation and revealing new physics beyond the Standard Model. There are many avenues to the CKM matrix elements open to lattice studies[1]. Figure 1 shows the Wolfenstein parameterization of the CKM matrix with some decays studied on the lattice. B semileptonic decays are of particular interest as ways of determining $|V_{ub}|$ and $|V_{cb}|$.

*Plenary talk presented at Lattice '95 Melbourne, Australia.

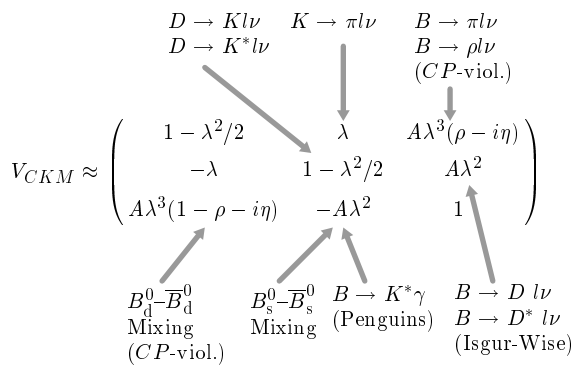


Figure 1. The CKM matrix in the Wolfenstein parameterization. Decay rate measurements yield CKM matrix elements provided hadronic matrix elements are known.

Figure 2. The (ρ, η) plane. The semicircular allowed region centered at $(0,0)$ (dotted lines) is from inclusive B semileptonic decays. The region between dashed lines is allowed by $B^0-\bar{B}^0$ mixing. The region between solid lines comes from CP -violating $K^0-\bar{K}^0$ mixing. Rosner[2].

The values of $|V_{ub}|$ and $|V_{cb}|$ from semileptonic decays place important constraints upon Wolfenstein parameters ρ and η . From Figure 1 the ratio of CKM elements is $\lambda\sqrt{\rho^2 + \eta^2}$ where λ is the sine of the Cabbibo angle. The ratio scaled by λ then defines a semi-circle centered at $(0,0)$ in the (ρ, η) plane. Uncertainties in the values of the CKM matrix elements widen the semicircle into the allowed region shown between the dotted arcs in Figure 2.

The figure also shows allowed regions in the (ρ, η) plane from $B^0-\bar{B}^0$ mixing and $K^0-\bar{K}^0$ mix-

ing. With more precise measurements of the CKM matrix elements the allowed regions will shrink. If all the regions no longer intersect this would indicate an inconsistency with the Standard Model. Uncertainties in hadronic matrix elements are now one of the largest sources of uncertainty for CKM matrix elements.

The ratio $|V_{ub}|/|V_{cb}|$ is now best determined by looking at the lepton energy spectrum for inclusive decays in the end-point region above the charm production limit[3,4]. This ratio depends upon theoretical form factors. Using current form factor models, the Particle Data Group[5] quotes $|V_{ub}|/|V_{cb}| = 0.08 \pm 0.02$ where the 25% error is due to combined statistical and theoretical uncertainties. Three-family unitarity of the CKM matrix and constraints from other CKM element measurements yield $|V_{ub}|$ values that range from 0.002 to 0.005 at the 90% confidence level. Thus, $|V_{ub}|$ is only known to within a factor of two.

The CLEO II collaboration has recently reported the first exclusive measurements for B light-meson semileptonic decay modes[6]. These measurements promise better methods of determining $|V_{ub}|$. Exclusive branching ratios determinations also require form factors as theoretical inputs. With current models the CLEO results have an uncomfortably large theoretical uncertainty. Hence, there is an essential need for reliable hadronic matrix elements. Given the phenomenological importance of V_{ub} , light-meson decays modes for the B meson deserve high priority in lattice studies.

The motivation for using the lattice is clear: it provides a direct numerical solution of QCD. At present, the lattice is the only systematically improvable, nonperturbative calculation method for QCD. Lattice technology for semileptonic decays is already well established[7]. Systematic errors must be understood to obtain reliable results from the lattice. Lattice discreteness is a source of systematic errors. Discretization errors for heavy quarks and momentum dependent errors are two important potential sources of error considered in Section 2.

Full $O(a)$ improvement for on-shell matrix elements with arbitrary-mass four-component quarks is discussed. Improved matrix elements

for bottom quarks can be studied on present lattices. Improvement increases the reliability of lattice calculations and allows coarser lattices to be used. Computations then become faster and cheaper. Less costly numerical calculations make it cost effective to do systematic studies of other sources of error.

Section 2.4 discusses momentum dependent errors. Estimates for momentum dependent errors in $O(a)$ -improved matrix elements on present lattices show that errors are probably less than 20% for momenta below 1 GeV/c. Reducing these errors would require smaller lattice spacings, adding $O(a^2)$ improvements to the quark action or extrapolations to zero lattice spacing at fixed physical momentum.

Section 3 is a survey of D decays on the lattice. Maximum meson recoil momenta in the D rest frame are below 1 GeV/c for semileptonic decays. Momentum dependent errors are then probably below 20% in present studies. Hence, form factors at maximum recoil momentum ($q^2 = 0$) can be extracted. A summary of lattice $D \rightarrow K$ and $D \rightarrow K^*$ form factors however, shows no trend with lattice spacing. Therefore, high precision tests for lattice spacing dependence are still needed.

Light-meson decay modes of the B are considered in Section 4. On present lattices, one approach to B decays is to study D decays and then to extrapolate, guided by heavy quark symmetry, to the B . Heavy-quark scaling of hadronic matrix elements is tested by calculating $O(a)$ -improved matrix elements for charm, bottom and static quarks. Matrix elements vary smoothly with quark mass. Therefore, when heavy quark symmetry is used to find B matrix elements, interpolations including static matrix elements are apt to be more reliable than extrapolations based on charm results alone.

Light mesons have a maximum recoil momentum of 2.6 GeV/c in B decays. Present B calculations are then restricted to only a fraction of the full momentum range. Predictions at large recoil momenta are then potentially unreliable. Differential decay rates and partial widths are suggested as useful quantities that can be reliably calculated with present lattices.

Section 5 reports upon decays with heavy hadron final states. Studies have focused upon mesons in order to understand $B \rightarrow D$ decays and extract $|V_{cb}|$. Baryon decays are now also under study. Baryons offer a new laboratory for heavy quark symmetry studies – including baryon Isgur-Wise universal form factors. Finally, two studies of Heavy Quark Effective Theory on the lattice are discussed. One study examines nonperturbative renormalization for lattice Heavy Quark Effective Theory while the second demonstrates a dramatic reduction in statistical noise when using optimized wavefunctions in calculations of the meson Isgur-Wise function.

2. ARBITRARY-MASS QUARKS

A quark is considered heavy when $m_0 \gg \Lambda_{QCD}$ as is the case for charm and bottom quarks. Wilson and Sheikholeslami-Wohlert (SW) heavy quarks are widely used in matrix element studies. On present lattices heavy-quark masses are typically a large fraction of the lattice cutoff $m_0 \gtrsim 1/a$. Errors arising from the discrete lattice can then be important. Standard Wilson quarks have $O(a)$ errors in matrix elements. Since decreasing the lattice spacing so that $am_0 \ll 1$ for a bottom quark is extremely costly, improvements which remove discretization errors on present lattices become an attractive alternative. This section focuses on a method for systematically removing lattice-spacing errors in four-component quarks of arbitrary mass.

Lattice-spacing errors can be observed in results for pseudoscalar decay constants. Figure 2 shows decay constants from a study using both Wilson and SW quarks on a lattice where the D -meson mass is $am_D \sim 1$ [8]. Wilson results are indicated by the diamond symbols in the figure. Conventional Wilson quarks incorrectly lead to $af\sqrt{am} = 0$ in the infinite-mass limit. Hence discretization errors overwhelm Wilson quarks at large masses. The figure shows that extrapolations of Wilson results from the D to the B are apt to be unreliable.

Errors in on-shell matrix elements can be reduced systematically by improving the lattice action and currents. $O(a)$ (Clover) improvement

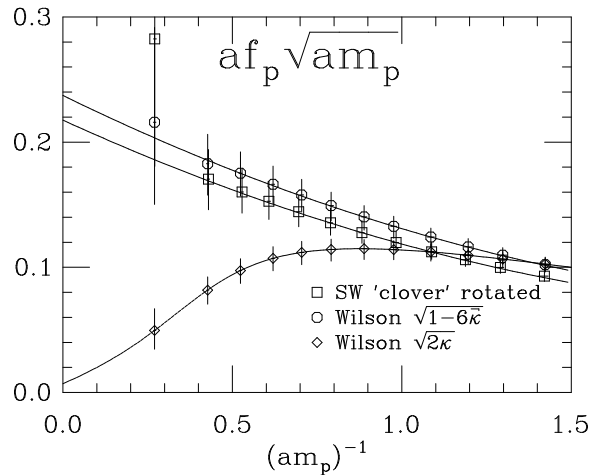


Figure 3. The quantity $af_p\sqrt{am_p}$ for heavy mesons. Three types of quarks are compared: conventional Wilson quarks (diamonds), improved Wilson quarks (octagons) and Clover quarks (squares). At large mass conventional Wilson quarks have large discretization errors. The D meson mass is $(am_D)^{-1} \approx 1$ on this lattice.

for light quarks is based upon the SW action[9]. The square symbols in Figure 2 denote Clover decay constants. Clover results extrapolate to an infinite-mass limit closer to the static value $af\sqrt{am} \approx 0.32$ indicating a sizable reduction in discretization errors at large mass compared to Wilson quarks.

Consider again the Wilson results. Large discretization errors are apparently removed by adopting an unconventional wavefunction renormalization for Wilson quarks[10,11]. Results for reinterpreted Wilson quarks (circles in Figure 2) also have an infinite-mass limit in better agreement with the static result. With the unconventional wavefunction renormalization the correct free-field quark propagator is recovered at infinite-mass. Since improvement is possible in both heavy and light limits, the Fermilab group then investigated the possibility of improvements for quarks of arbitrary mass.

The Fermilab program improves arbitrary-mass four-component quarks[12]. It is equiva-

lent to the usual improvements for light quarks and to the static approximation at infinite mass. Fully $O(a)$ -improved quarks are obtained using the SW action and improved currents. Bottom quarks can be put on existing lattices without $O(a)$ errors. Heavy Wilson and SW quarks are used successfully to study γ -onia[13]. In B -decay studies uncertainties due to extrapolations in the heavy-quark mass can be eliminated and calculations become cheaper and faster since present lattices can be used. Computational savings can then be used to remove remaining discretization errors by repeating calculations at several lattice spacings.

2.1. The Action

The $O(a)$ quark action in the Fermilab formalism is a sum of three terms:

$$S_f = S_0 + S_B + S_E. \quad (1)$$

Term S_0 has dimension-three and -four operators and a dimension-five Wilson operator to eliminate doublers:

$$\begin{aligned} S_0 = & m_0 \int \bar{\Psi}' \Psi' + \int \bar{\Psi}' \frac{1}{2} (1 + \gamma_0) D_0^- \Psi' \\ & - \int \bar{\Psi}' \frac{1}{2} (1 - \gamma_0) D_0^+ \Psi' + \zeta \int \bar{\Psi}' \vec{\gamma} \cdot \vec{D} \Psi' \\ & - \frac{1}{2} a r_s \zeta \int \bar{\Psi}' \Delta_s^{(2)} \Psi'. \end{aligned} \quad (2)$$

Operators D_μ^\pm are the forward (+) and backward (-) first differences, D_μ is the central difference and $\Delta_s^{(2)}$ is the spatial laplacian. By setting $r_s = 1$ and $\zeta = 1$ action S_0 becomes the Wilson action. The action is asymmetric in space and time when $\zeta \neq 1$.

The chromomagnetic and chromoelectric terms are:

$$S_B = -\frac{i}{2} a c_B \zeta \int \bar{\Psi}' \vec{\Sigma} \cdot \vec{B} \Psi' \quad (3)$$

$$S_E = -\frac{1}{2} a c_E \zeta \int \bar{\Psi}' \vec{\alpha} \cdot \vec{E} \Psi'. \quad (4)$$

In contrast to the light-quark action where $c_B = c_E$ and $S_B + S_E$ is ‘‘clover’’ term, here c_B and c_E may be unequal.

Parameters r_s , ζ , c_B and c_E are functions of the coupling; tree-level values are known. Higher-order corrections can be obtained perturbatively.

These parameters are also functions of quark mass. The mass dependence is treated to all orders.

Values $r_s = 1$, $\zeta = 1$ and $c = c_B = c_E$ are used for light quarks. With $c = 1$ the action is the tree-level SW action; tadpole improvement increases c to between 1.4 and 1.5 on typical lattices. The tadpole-improved SW action leads to fully $O(a)$ -improved light quarks. $O(a)$ improvement is still obtained for heavy quarks provided currents and the physical mass are suitably defined.

2.2. Physical Heavy-Quark Masses

In the non-relativistic limit, the Hamiltonian corresponding to S_f is

$$\begin{aligned} H \simeq \bar{\Psi} \left(M_1 + \gamma_0 A_0 - \frac{\vec{D}^2}{2M_2} - \frac{i\vec{\Sigma} \cdot \vec{B}}{2M_B} \right. \\ \left. - \gamma_0 \frac{[\vec{\gamma} \cdot \vec{D}, \vec{\gamma} \cdot \vec{E}]}{8M_E^2} \right) \Psi \end{aligned} \quad (5)$$

where Ψ is the physical field defined in Equation 8. This looks like the Pauli Hamiltonian; M_1 , M_2 , M_B , and M_E however are functions of m_0 . This Hamiltonian describes a non-relativistic quark when $M_2 = M_B = M_E$. For both Wilson and SW quarks, when $am_0 \gtrsim 1$ the kinetic mass, M_2 , and the rest mass, M_1 , are significantly different. Since M_1 is unimportant for non-relativistic quarks, M_2 should then be considered the physical mass.

The Hamiltonian is a useful guide for estimating errors for non-relativistic quarks. Systematic errors will arise if M_B and M_E do not equal M_2 . At tree-level, when $am_0 \gtrsim 1$ Wilson quarks have $M_B > M_2$ while SW quarks have $M_B \simeq M_2$. Therefore, from Equation 5, Wilson quarks can be expected to correctly reproduce only spin-averaged energy levels while SW quarks should also approximate spin-dependent features.

Physical quark masses can be found non-perturbatively in γ -onia by using the non-relativistic energy dispersion relation

$$E_1^{NR} = m_1 + \frac{\vec{p}^2}{2m_2} + \dots \quad (6)$$

The meson kinetic mass, m_2 , and the rest mass, m_1 , differ significantly when $am_0 \gtrsim 1$ for Wil-

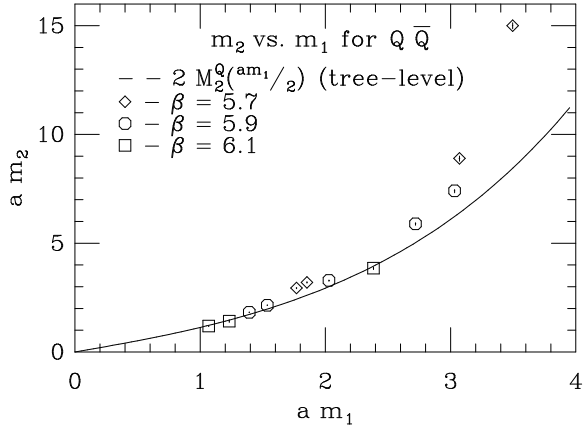


Figure 4. Meson kinetic mass, m_2 , as a function of the rest mass, m_1 in -onia. Points are lattice determinations using the energy dispersion relation. The curve is based upon the tree-level expression for the quark kinetic mass in terms of the rest mass.

son and SW quarks. Charm and bottom quark masses are determined by matching the physical mass and m_2 . Spin-averaged levels are used; the physical lattice spacing may be found using the $1P$ - $1S$ mass splitting.

Figure 4 shows am_2 and am_1 values obtained for three lattice spacings using SW quarks. Numerical results agree well with the curve[14] which is based on the tree-level functional relation between quark masses M_2 and M_1 . Differences between numerical results and tree-level predictions are, in part, due to higher-order corrections. One-loop corrections to quark masses are being computed[15]. The figure shows that the rest mass systematically underestimates the physical mass. At $\beta = 6.1$, M_2/M_1 is about 1.2 for the charm quark and 2.8 for the bottom quark. Using the rest mass to determine the physical mass rather than the more physical kinetic mass introduces a systematic error into heavy-quark calculations.

2.3. Currents

Fully $O(a)$ -improved matrix elements require $O(a)$ -improved currents. Physical fermion operators, Ψ , appear in renormalized currents. These

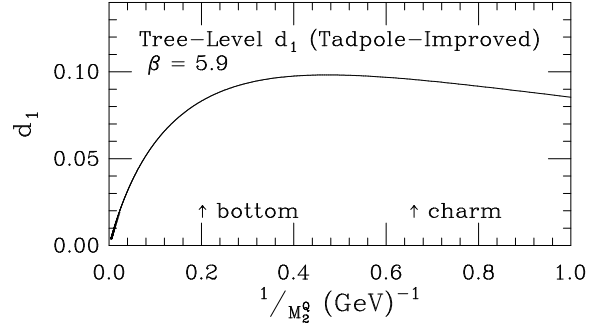


Figure 5. Tadpole-improved tree-level values of coefficient d_1 plotted as a function of $1/M_2^2$ for $\beta = 5.9$. Coefficient d_1 equals zero in the infinite- and zero-mass limits and is typically largest between charm and bottom.

fields are constructed from fields Ψ'' , which appear in the hopping parameter form of action S_f . Fields Ψ are given by[16]

$$\hat{\Psi} = \left[1 + ad_1(m_0, g^2) \vec{\gamma} \cdot \vec{D} + O(a^2) \right] \Psi'' \quad (7)$$

$$\Psi = \sqrt{2\kappa} \exp(aM_1/2) \hat{\Psi}. \quad (8)$$

The three-gradient term is an $O(a)$ correction to the current; the exponential factor is a correction in all-orders of am_0 .

Coefficient d_1 depends upon the action and is a function of the coupling and quark mass. Figure 5 shows d_1 as a function of $1/M_2^2$ for tadpole-improved SW quarks at $\beta = 5.9$. At tree-level, d_1 vanishes in both zero- and infinite-mass limits. The correction is typically largest between charm and bottom. At $\beta = 5.9$, lattice results show that f_D increases by about 7% when the three-gradient term is included in the current.

In Equation 8 the factor $\exp(aM_1/2)$ appears in addition to the conventional $\sqrt{2\kappa}$ factor for Wilson and SW quarks. This factor removes large discretization errors when $am_0 \gtrsim 1$. Its effect upon Wilson decay constants is seen in Figure 2. To $O(am_0)$ this factor is equivalent, at tree-level, to the Clover rotation used to improve light-quark currents. The factor becomes $\sqrt{1 - 6\kappa}$ using the tree-level expression for the rest mass and $\sqrt{1 - 6u_0\kappa}$ with tadpole improvement. The average plaquette or kappa critical is typically used

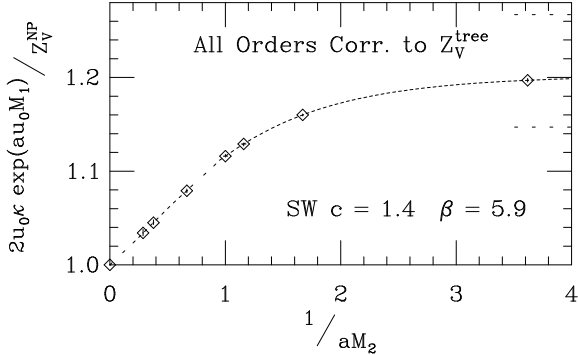


Figure 6. All-order corrections beyond tree-level for the vector current renormalization. Corrections have a mild dependence upon quark mass. They are consistent with perturbation theory for small masses. At infinite mass higher-order corrections are zero and the tadpole-improved tree-level renormalization yields the exact result.

to estimate u_0 [17].

An $O(a)$ -improved current coupling quarks Q and q has the form

$$J^\mu = \bar{\Psi}_Q \Gamma^\mu \Psi_q = Z_J(m_0^Q, m_0^q, g^2) \bar{\Psi}_Q \Gamma^\mu \hat{\Psi}_q \quad (9)$$

where the fields are given in Equations 7 and 8. Matrix Γ^μ equals γ^μ for a vector current and $\gamma^\mu \gamma^5$ for an axial current. Renormalization Z_J matches the lattice current to the continuum.

With tadpole improvement, Z_J becomes

$$Z_J = \sqrt{2\tilde{\kappa}_Q 2\tilde{\kappa}_q} \exp \left[\frac{1}{2} (a\tilde{M}_1^Q + a\tilde{M}_1^q) \right] \tilde{Z}_\Gamma \quad (10)$$

where \tilde{Z}_Γ is the vertex correction. Here, $\tilde{\kappa} \equiv u_0 \kappa$ and \tilde{M}_1 denotes tadpole-improved M_1 . Z_J keeps this form to any order in g^2 . For example, at $O(g^2)$ expansions $\tilde{M}_1 = \tilde{M}_1^{[0]} + g^2 \tilde{M}_1^{[1]}$ and $\tilde{Z}_\Gamma = 1 + g^2 \tilde{Z}_\Gamma^{[1]}$ appear in Equation 10. The higher-order corrections to Z_J are also functions of the quark masses.

The mass dependence of higher-order terms in Z_J can be checked non-perturbatively for the vector current by examining the charge normalization of three-point functions. Figure 6 shows the ratio of the tree-level renormalization factor, Z_V^{tree} , and the nonperturbative factor, Z_V^{np} ,

versus $1/M_2$ for tadpole-improved SW quarks at $\beta = 5.9$. Terms in Z_V^{np} beyond tree level cause this ratio to differ from unity. The figure shows that higher-order corrections change Z_V^{tree} by at most 20% and that light-quark corrections are largest. One-loop corrections of around 20% are expected for light quarks at $\beta = 5.9$. Note that renormalization Z_V^{tree} is exact in the static limit[18]. Thus, higher-order corrections depend smoothly on mass and yield the expected results in the light- and infinite-mass limits.

The Wuppertal Group[19] has also checked the renormalization in Equation 10 non-perturbatively. They look at ratios of the local-current three-point function over the conserved-current three-point function. They test Equation 10 as function of quark mass using flavor-conserving currents, heavy-light currents, and currents carrying momentum. The last two cases are important tests of the current renormalization for semileptonic decays.

They find that Z_V^{tree} , given by Equation 10, is in reasonable agreement with the nonperturbative determination of Z_V for the three cases studied. Because of mass-dependent higher-order terms, exact agreement between the nonperturbative renormalization and Z_V^{tree} is not expected. In contrast to Equation 10, mass-independent renormalization using the perturbative result for light quarks leads to poor agreement with the nonperturbative results for heavy quarks.

2.4. Momentum Dependent Errors

With fully $O(a)$ -improved actions and currents $O(a\vec{p})$ errors are removed from matrix elements. Since improvement is carried out for on-shell quarks at rest, however, momentum dependent discretization errors are still a concern at large momenta $|a\vec{p}| \gg 0$. It is then important to consider the effect of momentum dependent errors in semileptonic decays. Tree-level errors in quark matrix elements can be determined analytically by comparing infinite-volume lattice matrix elements and continuum matrix elements. Errors in the quark matrix elements can then serve as a guide to estimating errors in hadronic matrix elements.

Consider matrix elements for an external vector

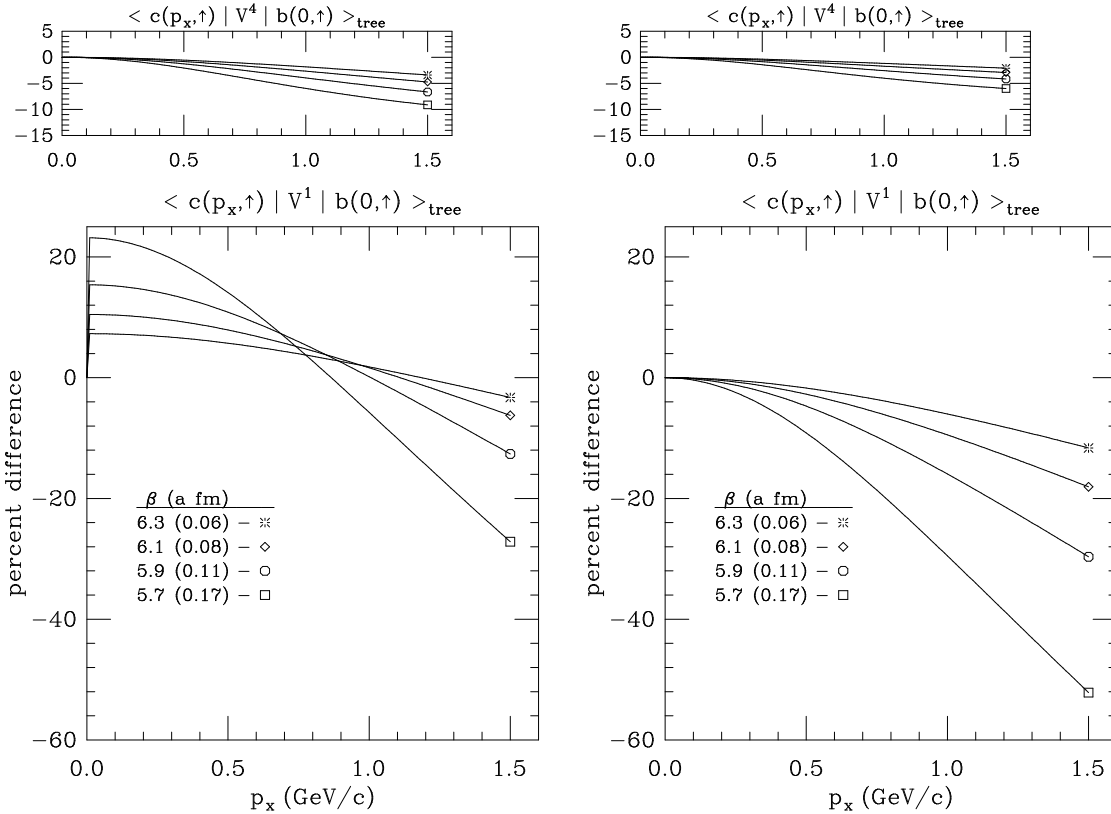


Figure 7. Momentum dependent errors in tree-level quark matrix elements $\langle c(p_x, \uparrow) | V^\mu | b(\vec{0}, \uparrow) \rangle_{\text{tree}}$ for typical lattice spacings. Errors are shown as a function of the charm-quark physical momentum. Plots show errors in temporal (top) and spatial (bottom) matrix elements. Currents are the local current (left) and the $O(a)$ -improved current (right).

current $\langle q(p_f, \sigma_f) | V^\mu | Q(p_i, \sigma_i) \rangle$ where the current is defined in Equation 9. Matrix elements for the local current ($d_1 = 0$ in Equation 7) and for the $O(a)$ -improved current are calculated. Wilson quarks with equal kinetic and physical masses are used. For simplicity, the initial quark is at rest. This should be a good approximation to a heavy quark decaying within a meson at rest. Since matrix elements are independent of the mass of the at-rest quark, error estimates are the same for charm and bottom decays. Here, the initial quark is taken to be a bottom quark. Only on-axis recoil momenta are considered for the final quark.

Figure 2.4 shows the relative error in lattice matrix elements with a charm-quark final state

as a function of the physical momentum. Plots on the left show errors for the local current, while those on the right show errors for the $O(a)$ -improved current. Upper plots correspond to temporal matrix elements while the lower plots show spatial matrix elements. Plots show typical lattice spacings in the range 0.17 to 0.06 fm.

Errors change more systematically with momentum with the improved current. Hence discretization errors in hadronic matrix elements are likely to be under better control at small momenta with the improved current. Note however that even with full $O(a)$ improvement errors in spatial matrix elements may still be of order 20% at $|\vec{p}| = 1.24$ GeV/c on a $\beta = 5.9$ lattice. A mo-

momentum of 1.24 GeV/c corresponds to two units of lattice momentum on a two fermi lattice. Errors can be reduced by adding $O(a^2)$ improvements to the action and currents. Note however that precision matrix elements may still be obtainable in the presence of sizable discretization errors by extrapolating lattice matrix elements to zero lattice spacing at fixed physical momenta. The feasibility of this approach hinges upon using suitable techniques to control statistical noise in lattice correlators with momentum[20].

3. D DECAYS

Semileptonic decays on the lattice were pioneered with studies of D mesons[21,22]. D decays continue to be an active area of investigation[23, 24,25,26,28]. At this conference the Los Alamos[27] and Wuppertal[19] groups presented updates for their D studies. Charm decays are an interesting laboratory for QCD and serve as a first step towards the study of B decays. D -decay experiments provide a basis for comparison in lattice studies. Experimental checks for D decays are an important way of checking systematic errors in lattice calculations.

Experimental information for D decays has grown steadily since the first lattice calculations. Nevertheless, the K and K^* recoil momentum distributions are still not well known[29]. Instead, pole dominance is typically used to extract form factor values at maximum recoil momentum corresponding to $q^2 \equiv (p_D - p_K)^2 = 0$. For the K , the location of the pole can also be determined from the data. Experiments find pole masses consistent with identifying the D_s^* as the dominant pole. For K^* , pole masses are fixed to the D_s^* and D_s^{**} masses and form factor ratios $R_V = V(0)/A_1(0)$ and $R_2 = A_2(0)/A_1(0)$ are found. Individual vector form factors are then found by assuming the branching ratio depends predominantly on A_1^2 . Hence experimental evidence for pole dominance in D decays is indirect.

Lattice calculations for D decays cover the whole range of recoil momentum. Statistical and systematic errors at maximum recoil are important to estimate since D results are traditionally presented as form factors at maximum re-

coil. In the D rest frame the maximum kaon momentum is 0.86 GeV/c while the maximum pion momentum is 0.93 GeV/c. Statistical errors at such momenta can be minimized by using good source operators for moving mesons. With ~ 300 gauge configurations statistical errors below 10% are likely for the whole recoil-momentum range.

Momentum dependent errors at maximum recoil can be estimated from errors in tree-level quark matrix elements. Errors in $f_+^K(0)$ are predicted to be around 10% with $O(a)$ -improved quarks at $\beta = 5.9$. This and other discretization errors can be reduced by working on a finer lattice. With improved actions, however, extremely fine lattice spacings are not necessary. A series of faster less costly computations on relatively coarse lattice spacings can be done. Remaining discretization errors are then removed by extrapolation to zero lattice spacing[30].

Table 1 is a summary of D form factors at $q^2 = 0$ obtained in lattice studies. Statistical errors are shown with estimates, when given, for systematic uncertainties. Best estimates of form factors from experimental studies are shown for comparison[29]. To investigate lattice-spacing errors, lattice spacings, lengths and the quark action used in each study are listed in the table. Lattice results are mostly within two sigma of the experimental values. Unfortunately, while statistical errors for f_+^K are typically below 15% statistical errors for the other form factors tend to be larger. Hence, from the tabulated results it is difficult to determine how lattice-spacing errors affect form factors. Higher precision studies of D decays are needed. Comparison with experiment will be an important test of whether systematic errors are under control.

Since discrete lattice momenta typically bracket $q^2 = 0$, the form factors in Table 1 are obtained by interpolation or, in cases where statistical errors were too large, by extrapolation over a limited range of recoil momentum. In practice, pole dominance provides a simple means of smoothly interpolating lattice results.

The Los Alamos[27] and Wuppertal[19] groups both test possible interpolation functions – including pole dominance forms. The Los Alamos group note that at leading order in $1/m_c$ the

Table 1

$D \rightarrow K l \nu$ and $D \rightarrow K^* l \nu$ form factors at $q^2 = 0$. Experimental averages (**EX**) and a summary of lattice results (**LA**) are shown. Lattice spacings, **a**, lengths, **L** (both in fm) and the quark action (**Ac**) used in each study are also shown.

Reference	a	L	Ac	$f_+(0)$	$V(0)$	$A_1(0)$
EX Average [29]				0.75 ± 0.03	1.1 ± 0.2	0.56 ± 0.04
LA LMMS [23]	.095	1.0	W	0.63 ± 0.08	0.86 ± 0.10	0.53 ± 0.03
BKS [24]	.095	2.3	W	$0.90 \pm 0.08 \pm 0.21$	$1.43 \pm 0.45 \pm 0.49$	$0.83 \pm 0.14 \pm 0.28$
ELC [25]	.055	1.3	W	$0.60 \pm 0.15 \pm 0.07$	0.86 ± 0.24	0.64 ± 0.16
UKQCD [26]	.071	1.7	SW	$0.67^{+0.07}_{-0.08}$	$1.01^{+0.30}_{-0.13}$	$0.70^{+0.07}_{-0.10}$
LANL [27]	.095	3.0	W	0.71 ± 0.04	1.28 ± 0.07	0.72 ± 0.03
LAT-APE[28]	.095	1.7	SW	0.78 ± 0.08	1.08 ± 0.22	0.67 ± 0.11
W'tal[19]	.064	1.5	W	$0.71 \pm 0.12^{+0.10}_{-0.07}$	$1.34 \pm 0.24^{+0.19}_{-0.14}$	$0.61 \pm 0.06^{+0.09}_{-0.07}$
Reference	a	L	Ac	$A_2(0)$	$V(0)/A_1(0)$	$A_2(0)/A_1(0)$
EX Average [29]				0.40 ± 0.08	1.89 ± 0.25	0.73 ± 0.15
LA LMMS [23]	.095	1.0	W	0.19 ± 0.21	1.6 ± 0.2	0.4 ± 0.4
BKS [24]	.095	2.3	W	$0.59 \pm 0.14 \pm 0.24$	$1.99 \pm 0.22 \pm 0.33$	$0.7 \pm 0.16 \pm 0.17$
ELC [25]	.055	1.3	W	$0.40 \pm 0.28 \pm 0.04$	1.3 ± 0.2	0.6 ± 0.3
UKQCD [26]	.071	1.7	SW	$0.66^{+0.10}_{-0.15}$	$1.4^{+0.5}_{-0.2}$	0.9 ± 0.2
LANL [27]	.095	3.0	W	0.49 ± 0.09	1.78 ± 0.07	0.68 ± 0.11
LAT-APE[28]	.095	1.7	SW	0.49 ± 0.34	1.6 ± 0.3	0.7 ± 0.4
W'tal[19]	.064	1.5	W	$0.83 \pm 0.20^{+0.12}_{-0.08}$		

heavy quark symmetry relation between D form factors f_+ and f_0 appears to be incompatible with both form factors having a pole form. They find f_+^K favors a pole mass lighter than the D_s^* mass while f_0 yields the expected pole mass. To determine $f_+^K(0)$ they use the pole form giving the lighter effective pole rather than fixing the pole mass to the D_s^* mass.

Although functions inspired by pole dominance are commonly used for interpolations of lattice D form factors it is important to remember that how adequately pole dominance describes D decays or especially B decays is not known.

4. B DECAYS TO LIGHT MESONS

The light-meson decay modes for the B are especially important calculations for the lattice now that the CLEO II collaboration has branching ratios for the pion and rho[6]. With a sample of 2.6 million $B \bar{B}$ decays they find branching ratios

(scaled by $\times 10^{-4}$)

$$\mathcal{B}(B^0 \rightarrow \pi^- l^+ \nu) = \begin{array}{l} 1.34 \pm 0.35 \pm 0.28 \text{ (ISGW)} \\ 1.63 \pm 0.46 \pm 0.34 \text{ (BSW)} \end{array}$$

$$\mathcal{B}(B^0 \rightarrow \rho^- l^+ \nu) = \begin{array}{l} 2.28 \pm 0.36 \pm 0.59 \text{ }^{(+0.00)}_{(-0.46)} \text{ (ISGW)} \\ 3.88 \pm 0.54 \pm 1.01 \text{ }^{(+0.00)}_{(-0.78)} \text{ (BSW)} \end{array}$$

The first error for each ratio is statistical and the second is systematic. The third error for the rho is the uncertainty due to non-resonant $\pi\pi$ contributions. These branching ratios depend upon theoretical input for the efficiency calculation. The branching ratios above result when the ISGW[31] and the WSB[32] quark models are used for efficiencies. Differences between the models indicate that theoretical uncertainties in the hadronic matrix elements are a substantial source of error. Note that reliable hadronic matrix elements are even more important for determining $|V_{ub}|$.

Light decay modes are under investigation on the lattice [25,28,33,34,19]. These studies all use either standard Wilson or Clover[9] quarks. Be-

cause of concerns over discretization errors, direct calculations involve heavy mesons with masses around the D mass. Heavy quark symmetry is then used to guide extrapolations from the D system to the B meson.

Hadronic matrix elements for light-meson decay modes scale in the heavy-quark limit[35,36]. For example, consider decays $H \rightarrow \pi l\nu$. In the H -meson rest frame

$$\alpha_s(m_H)^{2/\beta_0} \frac{\langle \pi(\vec{p}_\pi) | V^\mu | H(\vec{0}) \rangle}{\sqrt{2m_H 2E_\pi}} \sim \mathcal{M}(p_\pi) \quad (11)$$

where \mathcal{M} is independent of the heavy-meson mass. The relation is not an equality since there are $O(1/m_H)$ corrections. In particular, the recoil momentum is assumed to be small $|\vec{p}_\pi|/m_H \ll 1$. Equation 11 relates D and B matrix elements with equal pion momentum. If $O(1/m_H)$ scale-breaking terms were small this expression would provide useful information about B decays from experimental data for D decays.

Form factor scaling relations follow from matrix element relations. For example, from Equation 11 one finds $f_+/\sqrt{m_H} \sim \gamma_+(1 + \delta_+/m_H)$ (modulo logarithms) where the linear $1/m_H$ scale-breaking term is now explicit. On the lattice, linear functions are typically used for extrapolations. In a pioneering study using this method the ELC group found $1/m_H$ terms which differ from zero by at most two sigma[25]. Statistical errors however did not exclude slopes as large as 1 GeV for $f_+/\sqrt{m_H}$ and 0.7 GeV for $A_1\sqrt{m_H}$. These statistical errors and possible systematic errors in heavy-quark extrapolations are sources of uncertainty in B -meson results.

The quantity $\langle \pi | V^\mu | H \rangle / \sqrt{2M_H 2E_\pi}$ in Equation 11 is obtained directly in lattice calculations when the heavy meson is at rest. The dependence upon heavy-quark mass has been investigated by the Fermilab group on a $\beta = 5.9$ lattice. Matrix elements were computed using fully $O(a)$ -improved charm and bottom quarks with strange-mass light quarks. Results were also obtained in the static approximation. Figure 8 shows the hadronic matrix elements parameterized by pion momentum and plotted versus $1/m_H$. Plot symbols and dashed curves distinguish pion momentum values. Momenta in lattice units are indi-

cated in the plots; one unit of momentum corresponds to 0.70 GeV/c. The plot on the left shows temporal matrix elements and on the right are x -component matrix elements. Matrix elements vary smoothly from charm to the static limit. Therefore in studies employing extrapolations from the D to the B , results are likely to be more reliable when static matrix elements are included so that B results are then obtained by interpolation.

Light-meson decay modes for the B have a maximum recoil momentum of 2.6 GeV/c compared to only 0.93 GeV/c for D decays. Concerns over momentum dependent discretization errors and statistical errors which increase rapidly with momentum limit current calculations to momenta around 1 GeV/c. Hence in contrast to D decays, B form factors at $q^2 = 0$ are far beyond the range of direct calculation. In addition, extrapolations to large recoil momenta are also likely to be unreliable. Extrapolations to large momenta can amplify small discretization errors which occur for small momenta. Also, extrapolations which assume pole dominance for the B introduce an unknown degree of model dependence. Therefore it is best to focus upon quantities in B decays that can be directly calculated without extrapolations.

Differential decay rates and partial widths do not require large extrapolations in momentum. Consider the differential decay rate for $B \rightarrow \pi l\nu$

$$\frac{d\Gamma}{d|\vec{p}_\pi|} = 2m_B \frac{G_f^2 |V_{ub}|^2}{24\pi^3} \frac{|\vec{p}_\pi|^4}{E_\pi} |f_+^\pi(q^2)|^2. \quad (12)$$

Figure 9 shows this differential rate (less the momentum independent pre-factors) in a preliminary study of B decays by the Fermilab group. Statistical errors are shown by the solid-line error bars; larger (broken-line) error bars show momentum dependent errors estimated using tree-level quark matrix elements. In this $\beta = 5.9$ study statistical errors are below 10% and momentum dependent errors are estimated to be less than 15% below 1 GeV/c. Errors may then be small enough that extrapolations to zero lattice spacing are reliable enough to remove most discretization errors.

Results in Figure 9 are for strange-mass light quarks. Chiral extrapolations are necessary to

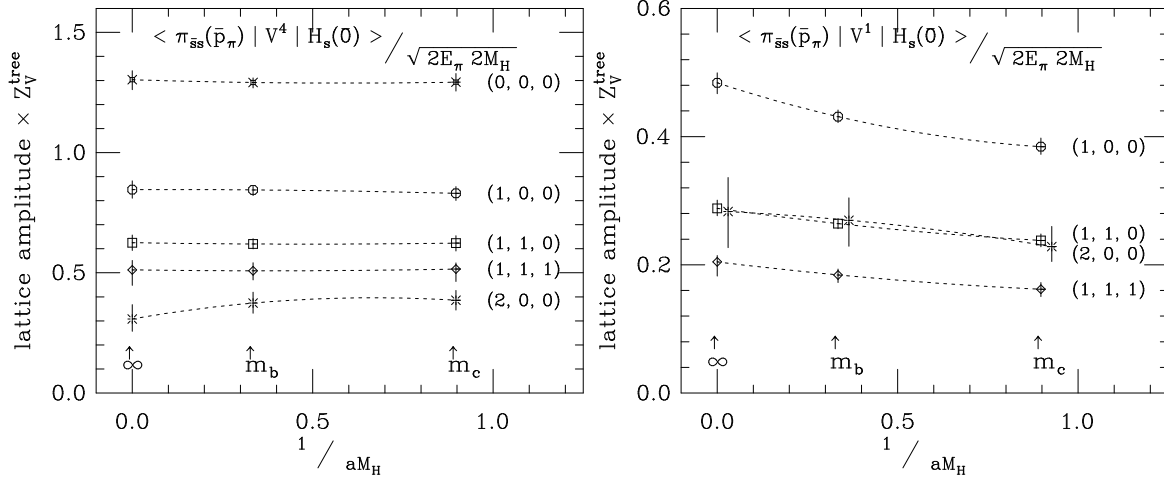


Figure 8. Hadronic matrix elements for static, bottom, and charm quarks at $\beta = 5.9$. The plot on the left shows temporal matrix elements. On the right are x -direction matrix elements which are proportional to the x -component of \vec{p}_π . Curves and distinct plot symbols indicate pion momenta which are shown in lattice units.

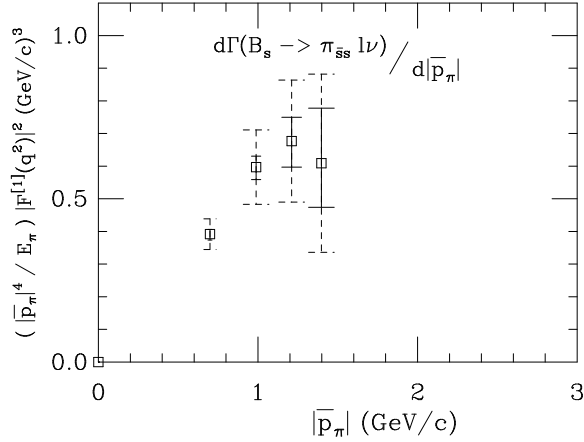


Figure 9. B -meson differential decay width for the light-pseudoscalar mode. Light-quark masses are approximately equal to the strange quark mass. Solid error bars are statistical errors. Estimated momentum dependent errors are shown by the larger broken-line error bars.

obtain decay rates for the physical pion. Chiral extrapolations of form factor f_+ at small pion momenta may be difficult since soft pion arguments suggest f_+ varies rapidly with pion mass in heavy-meson decays[36]. Note however variations in f_+ at small recoil momenta are suppressed by four powers of the momentum in the decay rate. Hence, chiral extrapolations of differential decay rates may be more robust than chiral extrapolations of form factors.

Partial widths can be obtained by smoothly interpolating between lattice differential decay rates values and then integrating. Partial widths obtained this way are expected to be relatively model independent for momenta within the range of direct lattice calculations. The UKQCD collaboration has found widths using this method for the vector decay mode[34]. Table 2 shows their results for differential decay rates and partial widths along with statistical errors. Chiral extrapolations have not been done and strange-mass light quarks are used. Note that at $q_0^2 = 14.4(\text{GeV}/c)^2$ which corresponds to $|\vec{p}_\rho| = 1.2 \text{ GeV}/c$ statistical errors are about 10% for the partial width. The authors point out that partial widths for the rho and pion decay modes from the lattice can be used to extract $|V_{ub}|$ in a model

Table 2

B -meson differential rates and partial widths for the light-vector decay mode. Momenta are in GeV/c. Width Γ is in units of $|V_{ub}|^2 \times 10^{-12}$ GeV. Strange-mass light quarks are used. UKQCD collaboration[34].

q_0^2	$d\Gamma/dq^2 _{q_0^2}$	$\int_{q_0^2}^{q_{max}^2} d\Gamma$
20.3	0.00	0.0
19.7 $\begin{pmatrix} +1 \\ -1 \end{pmatrix}$	0.19 $\begin{pmatrix} +3 \\ -2 \end{pmatrix}$	0.08 $\begin{pmatrix} +1 \\ -1 \end{pmatrix}$
17.5 $\begin{pmatrix} +2 \\ -2 \end{pmatrix}$	0.57 $\begin{pmatrix} +6 \\ -5 \end{pmatrix}$	0.9 $\begin{pmatrix} +1 \\ -1 \end{pmatrix}$
16.7 $\begin{pmatrix} +2 \\ -2 \end{pmatrix}$	0.58 $\begin{pmatrix} +9 \\ -6 \end{pmatrix}$	1.3 $\begin{pmatrix} +1 \\ -1 \end{pmatrix}$
15.3 $\begin{pmatrix} +3 \\ -3 \end{pmatrix}$	0.6 $\begin{pmatrix} +1 \\ -1 \end{pmatrix}$	2.3 $\begin{pmatrix} +2 \\ -2 \end{pmatrix}$
14.4 $\begin{pmatrix} +3 \\ -3 \end{pmatrix}$	0.8 $\begin{pmatrix} +2 \\ -1 \end{pmatrix}$	3.0 $\begin{pmatrix} +3 \\ -2 \end{pmatrix}$
charm threshold		
11.6	—	5.4 $\begin{pmatrix} +7 \\ -5 \end{pmatrix}$

independent way from exclusive B decay modes.

The CLEO II exclusive-mode analysis suggests that a sizable fraction of pions have momenta below 1.4 GeV/c. Hence exclusive partial widths from the lattice may in fact be a viable means of extracting $|V_{ub}|$. Minimizing errors in $|V_{ub}|$ will require adjusting the maximum recoil momentum limit in the partial width so as to minimize both lattice and experimental errors.

The most important task for semileptonic decay studies is improving the precision to which $|V_{cb}|$ is known. It is then important to eliminate potential sources of error. Extrapolations to large recoil momenta using present lattice results are unreliable. Differential decay rates and partial widths are likely to be more reliable and present lattice results in a form more useful to the experimental community.

5. DECAYS TO HEAVY HADRONS

Heavy-meson decay modes are studied to test non-perturbatively heavy quark symmetry and to provide theoretical input needed to extract $|V_{cb}|$ from B -meson decay rates. The study of these decay modes on the lattice is discussed in detail by Kenway[37] and by Lellouch[38]. This section provides an update in the form of results presented

at this conference.

The Isgur-Wise function (up to $O(1/m)$ corrections) has been extracted from QCD matrix elements calculated using Wilson and SW quarks[39,40]. Systematic error estimates for these calculations are not yet complete. Tree-level quark matrix elements however provide a way of estimating momentum-dependent errors. Note that according to Figure 2.4 relative errors are smaller for temporal matrix elements. Hence elastic form factors which require only temporal matrix elements are likely to yield the smallest momentum-dependent uncertainties for the Isgur-Wise function. The figure shows that tree-level errors are probably less than 10% for momenta below 1 GeV/c. It would be interesting to see how errors bias the determination of the Isgur-Wise slope at the zero-recoil point.

Another means of studying heavy quark symmetry is to formulate Heavy Quark Effective Theory (HQET) directly on the lattice[41]. At leading order lattice HQET (LHQET) describes an infinitely massive quark with arbitrary four-velocity. The lattice theory must be renormalized to match HQET.

At this conference, Mandula and Ogilvie investigate velocity renormalization[42]. In HQET the multiplicative renormalization of the heavy quark's four-velocity is actually a wavefunction renormalization. Lorentz symmetry is reduced on the lattice to hypercubic symmetry. Then, in LHQET additive shifts can also occur. These renormalizations have been computed perturbatively[43]. The perturbative expectations are compared with nonperturbative determinations of the renormalization coefficients from the lattice. In this pilot study, the coefficient of the term proportional to four-velocity is within one sigma of the one-loop value. Perturbative and lattice coefficients for terms cubic in the four-velocity were in complete disagreement however. Tadpole improvement of the LHQET action and a Lepage-Mackenzie treatment of perturbation theory[17] may help resolve these discrepancies.

The Kentucky group presented preliminary numerical results for the unrenormalized Isgur-Wise form factor in LHQET[44]. They find their variational method (MOST) for constructing optimal

wavefunctions can be effectively used in LHQET. MOST operators have good signal-to-noise ratios. With 32 gauge configurations statistical errors are around 5% while errors due to excited state contaminations are estimated to be 5%. These preliminary results encourage further study. Comparisons of the Isgur-Wise function directly computed using LHQET and the Isgur-Wise function extracted using finite-mass quarks will provide information about $O(1/m)$ errors.

Baryons containing one heavy quark are under study by the UKQCD collaboration[45]. Semileptonic decays of baryons may provide additional checks on CKM matrix elements. Baryons also offer additional tests of heavy quark symmetry. Consider the six form factors for $\Lambda_b \rightarrow \Lambda_c l \nu$. They are related to a single baryon Isgur-Wise function appearing in the heavy quark limit. The UKQCD collaboration presented preliminary results for the axial form factor which is expected to have small $O(1/m)$ corrections. They find little dependence upon $1/m$ when the heavy-quark mass is varied about the charm-quark mass.

Heavy hadron decays are important for determining $|V_{cb}|$. Lattice calculations provide valuable nonperturbative tests of heavy quark symmetry as well as Isgur-Wise form factors. HQET on the lattice is still being explored. In LHQET calculations statistical noise and poor ground-state isolation are important problems to be overcome. Highly optimal particle operators are then necessary.

6. REMARKS

Semileptonic decays provide important information about CKM matrix elements involving heavy quarks. Recent CLEO II results for the light-meson decay modes of the B are exciting since they promise better determinations of $|V_{ub}|$. Since reliable matrix elements are a crucial to this goal, B decays deserve high priority in lattice studies.

Systematic errors must be understood to obtain reliable results from the lattice. Discretization errors are an important source of uncertainty. Improvement does not require expensive lattices with drastically smaller lattice spacings to de-

crease discretization errors. Improvement is possible with arbitrary-mass four-component quarks. Bottom quarks can then be put on existing lattices. Extrapolations in the heavy-quark mass which are a potential source of systematic error in bottom-quark studies can then be eliminated.

With $O(a)$ improvement momentum dependent discretization errors in matrix elements are still a concern on present lattices for momenta above 1 GeV/c. Alternatives to drastically reducing the lattice spacing as a way of controlling momentum dependent errors include: $O(a^2)$ improvement, and extrapolations to zero lattice spacing at fixed physical momenta.

Present D decay calculations cover the full range of recoil momentum. Careful attention to sources of systematic error should lead to reliable matrix elements. Experimental data for D decays provide a basis for comparing lattice results. Checks for the D are important for testing that systematic errors are under control.

For light-meson decay modes of the B the maximum recoil momentum is greater than the largest momentum than can be confidently studied with present lattices. Attention should then be directed towards quantities that can be reliably determined. Differential decay rates and partial widths are a useful form for lattice results that do not require extrapolations to large recoil momenta. Partial widths from the lattice may offer a viable means of extracting $|V_{ub}|$ from the CLEO II exclusive decay measurements.

ACKNOWLEDGMENTS

I thank T. Bhattacharya, T. Draper, J. Flynn, C. McNeile and D. Richards for discussions and information about their work. I thank L. Gibbons and E. Thorndike for discussions concerning CLEO II exclusive decay results. I wish to thank my colleagues: B. Gough, G. Hockney, A. El-Khadra, A. Kronfeld, B. Mertens, T. Onogi and P. Mackenzie for an interesting and productive collaboration. Informative discussions with members of the FNAL theory group especially W. Bardeen, G. Burdman and E. Eichten are acknowledged. Fermilab calculations are performed on the ACPMAPS supercomputer. Fermilab is

operated by University Research Association, Inc. under contract with the U.S. Department of Energy.

REFERENCES

- [1] The reviews of C. Allton and A. Soni in these proceedings cover additional aspects of weak matrix elements.
- [2] J. Rosner, Proceedings of DPF'94, ed. Sally Seidel, World Scientific, 1994.
- [3] J. Bartelt *et al.*, *Phys. Rev. Lett.* **71** (1993) 4111.
- [4] H. Albrecht *et al.*, *Phys. Lett.* **B255** (1991) 297.
- [5] F.J. Gilman *et al.*, *Phys. Rev.* **D50 (Review of Particle Properties)** (1994) 1315.
- [6] L. Gibbons at Moriond '95, and CLEO Collaboration, CLEO CONF 95-09.
- [7] See reference [24] for example.
- [8] J.N. Simone, *Nucl. Phys.* **B (Proc. Suppl.) 30** (1993) 461.
- [9] G. Heatlie *et al.*, *Nucl. Phys.* **B352** (1991) 266.
- [10] P. Mackenzie, *Nucl. Phys.* **B (Proc. Suppl.) 30** (1993) 35.
- [11] A.S. Kronfeld, *Nucl. Phys.* **B (Proc. Suppl.) 30** (1993) 445.
- [12] A. El-Khadra A.S. Kronfeld and P.B. Mackenzie, in progress.
- [13] A. El-Khadra and B.P. Mertens, *Nucl. Phys.* **B (Proc. Suppl.) 42** (1995) 406.
- [14] S. Collins, PhD Thesis, Edinburgh University, 1993.
- [15] A.S. Kronfeld and B.P. Mertens, *Nucl. Phys.* **B (Proc. Suppl.) 34** (1994) 495.
- [16] A.S. Kronfeld, *Nucl. Phys.* **B (Proc. Suppl.) 42** (1995) 415.
- [17] G.P. Lepage and P.B. Mackenzie, *Phys. Rev.* **D48** (1993) 2250.
- [18] C. Bernard, *Nucl. Phys.* **B (Proc. Suppl.) 34** (1994) 47.
- [19] S. Güsken *et al.*, preprint HLRZ-95-38; S. Güsken these proceedings.
- [20] T. Onogi and J.N. Simone, *Nucl. Phys.* **B (Proc. Suppl.) 42** (1995) 434.
- [21] A. El-Khadra, C. Bernard and A. Soni, *Nucl. Phys.* **B (Proc. Suppl.) 9** (1989) 186.
- [22] V. Lubicz, G. Martinelli and C.T. Sachrajda, *Nucl. Phys.* **B356** (1991) 310.
- [23] V. Lubicz, G. Martinelli, M. McCarthy and C. T. Sachrajda, *Phys. Lett.* **274B** (1992) 415.
- [24] C. Bernard, A. El-Khadra and A. Soni, *Phys. Rev.* **D43** (1991) 2140; **D45** (1992) 869.
- [25] A. Abada *et al.*, *Nucl. Phys.* **B416** (1994) 675.
- [26] UKQCD collaboration – K.C. Bowler *et al.*, *Phys. Rev.* **D51** (1995) 4905.
- [27] T. Bhattacharya and R. Gupta, *Nucl. Phys.* **B (Proc. Suppl.) 42** (1995) 935; T. Bhattacharya these proceedings.
- [28] APE collaboration – C.R. Allton *et al.*, *Phys. Lett.* **B345** (1995) 513.
- [29] R. Morrison and J. Richman, *Phys. Rev.* **D50 (Review of Particle Properties)** (1994) 1565.
- [30] G.P. Lepage, these proceedings.
- [31] N. Isgur *et al.*, *PhysRev* **D39** (1989) 799
- [32] M. Wirbel, B. Stech and M. Bauer, *Z. Phys.* **C29** (1985) 637.
- [33] UKQCD collaboration – D.R. Buford *et al.*, *Nucl. Phys.* **B447** (1995) 425.
- [34] UKQCD collaboration – J.M. Flynn *et al.*, Southampton preprint SHEP 95-18.
- [35] N. Isgur and M. Wise, *Phys. Rev.* **D42** (1990) 2388.
- [36] G. Burdman *et al.*, *Phys. Rev.* **D49** (1994) 2331.
- [37] R.D. Kenway, *Nucl. Phys.* **B (Proc. Suppl.) 34** (1994) 153.
- [38] L. Lellouch, *Acta Phys. Polon.* **B25** (1994) 1679.
- [39] C.W. Bernard, Y. Shen and A. Soni, *Nucl. Phys.* **B (Proc. Suppl.) 34** (1994) 483.
- [40] UKQCD collaboration – S.P. Booth *et al.*, *Phys. Rev. Lett.* **72** (1994) 462.
- [41] J.E. Mandula and M.C. Ogilvie, *Nucl. Phys.* **B (Proc. Suppl.) 34** (1994) 480.
- [42] J.E. Mandula, these proceedings.
- [43] U. Aglietti, *Nucl. Phys.* **B421** (1994) 191.
- [44] T. Draper and C. McNeile, these proceedings.
- [45] D.G. Richards, these proceedings.

